

Interaction Patterns between *Potato Virus Y* and eIF4E-Mediated Recessive Resistance in the *Solanaceae*

Benoît Moury,^a Bénénger Janzac,^{a,b} Youna Ruellan,^a Vincent Simon,^a Mekki Ben Khalifa,^{c,d} Hatem Fakhfakh,^c Frédéric Fabre,^a Alain Palloix^b

INRA, UR407, Pathologie Végétale, Domaine Saint Maurice, Montfavet, France^a; INRA, UR1052, Génétique et Amélioration des Fruits et Légumes, Domaine Saint Maurice, Montfavet, France^b; Laboratoire de Génétique Moléculaire Immunologie et Biotechnologie, Faculté des Sciences de Tunis, Campus Universitaire El-Manar, Tunisia^c; Institut Supérieur de Biotechnologie de Béja, Béja, Tunisia^d

ABSTRACT

The structural pattern of infectivity matrices, which contains infection data resulting from inoculations of a set of hosts by a set of parasites, is a key parameter for our understanding of biological interactions and their evolution. This pattern determines the evolution of parasite pathogenicity and host resistance, the spatiotemporal distribution of host and parasite genotypes, and the efficiency of disease control strategies. Two major patterns have been proposed for plant-virus genotype infectivity matrices. In the gene-for-gene model, infectivity matrices show a nested pattern, where the host ranges of specialist virus genotypes are subsets of the host ranges of less specialized viruses. In contrast, in the matching-allele (MA) model, each virus genotype is specialized to infect one (or a small set of) host genotype(s). The corresponding infectivity matrix shows a modular pattern where infection is frequent for plants and viruses belonging to the same module but rare for those belonging to different modules. We analyzed the structure of infectivity matrices between *Potato virus Y* (PVY) and plant genotypes in the family *Solanaceae* carrying different eukaryotic initiation factor 4E (eIF4E)-coding alleles conferring recessive resistance. Whereas this system corresponds mechanistically to an MA model, the expected modular pattern was rejected based on our experimental data. This was mostly because PVY mutations involved in adaptation to a particular plant genotype displayed frequent pleiotropic effects, conferring simultaneously an adaptation to additional plant genotypes with different eIF4E alleles. Such effects should be taken into account for the design of strategies of sustainable control of PVY through plant varietal mixtures or rotations.

IMPORTANCE

The interaction pattern between host and virus genotypes has important consequences on their respective evolution and on issues regarding the application of disease control strategies. We found that the structure of the interaction between *Potato virus Y* (PVY) variants and host plants in the family *Solanaceae* departs significantly from the current model of interaction considered for these organisms because of frequent pleiotropic effects of virus mutations. These mutational effects allow the virus to expand rapidly its range of host plant genotypes, make it very difficult to predict the effects of mutations in PVY infectivity factors, and raise concerns about strategies of sustainable management of plant genetic resistance to viruses.

The interaction pattern between host and parasite genotypes has important consequences on their respective evolution and on issues regarding the application of disease control strategies. This pattern determines to a large extent the maintenance of genetic diversity in host and parasite populations (1), the structure of these populations in space and time (2, 3), and the evolution of parasite pathogenicity and host resistance (4).

Different models of host-parasite interaction and coevolution have been proposed (3, 5) (Fig. 1a to c). The gene-for-gene (GFG) model is the genetic system of interaction which was most frequently postulated for plant-pathogen interactions (4). In this system, a pathogen elicitor interacts with a host factor and triggers a specific defense reaction in the host which leads to the inhibition of infection. In contrast, the matching-allele (MA) model, initially proposed for an invertebrate immune system (5), describes a system where infection of a host by a parasite requires a specific match between some of their interacting factors. A pure MA model is an extreme form of biological specificity, where a parasite with a given genotype is only able to infect hosts belonging to a single genotype, and, reciprocally, hosts of a given genotype can only be infected by parasites of a single genotype (5). Compared to this one-to-one interaction pattern, a more relaxed model sup-

poses that a parasite with a given genotype is able to infect hosts belonging to a few genetically related genotypes (and vice versa). In that situation, the host-parasite interaction matrix is organized into interaction modules, where host and parasite genotypes belonging to the same module are more preferentially compatible with each other (i.e., hosts are infected and parasites are infectious) than with members of other modules.

The GFG, MA, and modular models correspond to interaction matrices that differ in the frequency and structure of compatibility cases (Fig. 1a to c). In a dynamic GFG coevolution, parasites adapt to a new resistance gene or allele in the host without losing their adaptations to older forms of host resistance. Accordingly, cross-infectivity, where a parasite with a given genotype is able to infect

Received 3 April 2014 Accepted 9 June 2014

Published ahead of print 18 June 2014

Editor: A. Simon

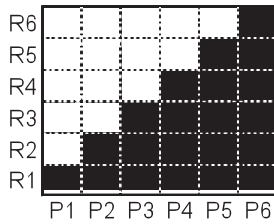
Address correspondence to Benoît Moury, moury@avignon.inra.fr.

Copyright © 2014, American Society for Microbiology. All Rights Reserved.

doi:10.1128/JVI.00930-14

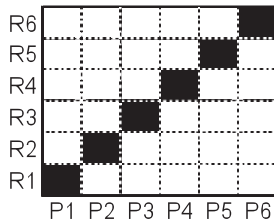
a. Gene for gene

(freq. = 0.58; nest. = 1.00; modul. = 0.17)



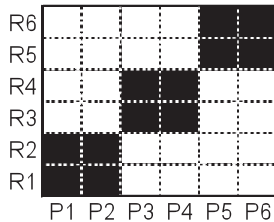
b. Matching allele

(freq. = 0.16; nest. = 0.37; modul. = 0.83)



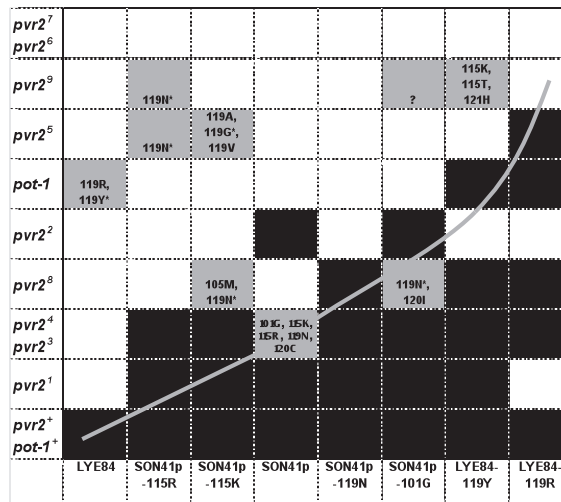
c. Modular

(nest. = 0.24; modul. = 0.67)



d. PVY VPg mutants

(freq. = 0.44; nest. = 0.80; modul. = 0.23)



e. Field pepper PVY isolates

(freq. = 0.52; nest. = 0.93; modul. = 0.18)

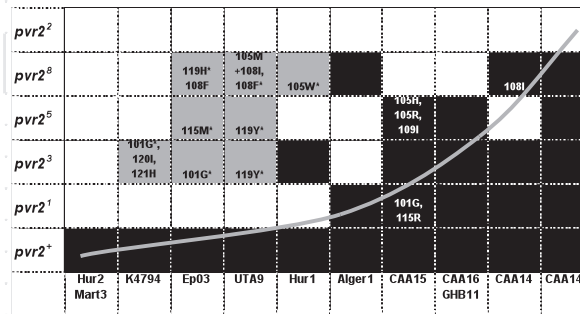


FIG 1 Interaction matrices between host and parasite genotypes. (a to c) Three theoretical interaction matrices between host genotypes carrying different resistance genes or alleles (R1 to R6) and parasite pathotypes (P1 to P6). Black boxes indicate infection of the host with the indicated genotype by the parasite with the indicated genotype, and white boxes indicate lack of infection. (d and e) Experimental interaction matrices between PVY variants (columns) and plants of *Capsicum annuum* or *Solanum habrochaites* with genotypes (rows) carrying different alleles at the *pvr2* or *pot-1* locus, respectively. Black boxes indicate infection of 100% of inoculated plants, whereas white boxes indicate no infection. Gray boxes indicate <100% infection and occurrence of additional mutations in the VPg pathogenicity factor. Amino acid substitutions observed in the VPg of the viral progeny are indicated within boxes. The question mark indicates that a single plant was infected, and no sequence was obtained for the VPg-coding region. Asterisks indicate PVY populations, almost all of which show secondary mutations in the VPg-coding region, that were chosen for back-inoculation in the same plant genotype. For all of them, all (25 of 25) back-inoculated plants were infected 15 days after inoculation. These matrices differ by the frequency of compatibility (infection) cases (freq) and the nestedness (nest; estimated with the algorithm of Rodríguez-Gironés and Santamaría [19]) and modularity (modul; estimated with an exhaustive search algorithm) of these compatibility cases. The rows and columns of matrices shown in panels d and e were ordered to evidence the significant nested pattern (gray curve) (Table 1). No frequency of compatibility cases is indicated for the modular model because it depends greatly on the size of modules.

hosts belonging to different genotypes, is frequent. A symmetrical situation occurs with hosts, where new resistance genes or alleles protect against recently evolved parasite genotypes and also against older parasite genotypes. As a result, the interaction matrix shows a nested, stair-like compatibility pattern (Fig. 1a). In contrast, under the MA model and, to a lesser extent, under the modular model, parasite mutations conferring infectivity to hosts with newly evolved resistance genes simultaneously abolish the capacity to infect older host genotypes. This model is characterized by rare cross-infectivity for parasites. The interaction matrix shows a modular pattern, where compatibility cases are concentrated along the diagonal. As a consequence, the interaction matrices corresponding to these different models can be distinguished by the frequency of compatibility cases, their nestedness (i.e., the

maximal degree of concentration of the compatibility cases in the lower right portion of the matrix that can be achieved after row and column permutation), and their modularity (i.e., the maximal degree of concentration of the compatibility cases into modules that group host and parasite genotypes). It is important to keep in mind that host-parasite interaction matrices where rows and/or columns are permuted are equivalent and that the total number of equivalent matrices obtained through row and/or column permutations becomes rapidly very large as the number of rows and columns increases, causing computational issues.

In plant-virus interactions, both the FFG and MA models have been postulated (4). The interaction matrix between pepper (*Capsicum* spp.) plants representing genotypes with different alleles at the *L* locus, conferring dominant resistance, and tobamoviruses

(genus *Tobamovirus*) shows a nested pattern which fits with the GFG model. Furthermore, the tobamovirus genotypes with the largest spectrum of infectivity show fitness costs in terms of accumulation in susceptible plant genotypes (6), a prediction of the GFG model. In contrast, interaction between plants with genotypes carrying eukaryotic initiation factor 4E or 4G (eIF4E or eIF4G, respectively)-mediated recessive resistance and different groups of viruses was assumed to correspond to an MA model. Indeed, in these pathosystems, infectivity depends on a direct physical interaction between a host factor (eIF4E or eIF4G) and a virus factor (most frequently, the genome-linked viral protein, or VPg) (7, 8). The most exhaustive study is that of the interaction between rice recessive resistance alleles at the *rymv1* locus (mainly alleles *rymv1-2* and *rymv1-3*) and *Rice yellow mottle virus* (RYMV; genus *Sobemovirus*) (9–11). As in the MA model, cross-infectivity was rare since among the RYMV isolates that could adapt to plants carrying the resistance alleles, 89% (34/38) were able to infect only genotypes with *rymv1-2* or only genotypes with *rymv1-3* (11). This “converse genetic barrier” for adaptation to *rymv1-2* and *rymv1-3* was later shown to be conferred by a particular mutation in the VPg of RYMV (9). However, given the small set of resistance alleles examined, it is presently not possible to obtain statistical evidence about the structure of this interaction matrix and to assign it to a GFG or MA model.

In this study, we examined the interaction pattern between 12 plant genotypes in the family *Solanaceae* carrying different eIF4E-mediated resistance/susceptibility factors and *Potato virus Y* (PVY; genus *Potyvirus*) genotypes. Although the mechanistic bases of virus infectivity and plant resistance in this system fit with the assumptions of the MA or modular model, these were rejected after the structure of the interaction matrix was analyzed. One reason was a particularly high frequency of pleiotropic cross-infectivity mutations in PVY conferring simultaneously an adaptation to the resistance controlled by several genes or alleles and contrasting with the rice-RYMV system. Such interaction patterns and the causative mutations in plants and viruses have important consequences in terms of resistance management.

MATERIALS AND METHODS

Plant material. Ten pepper (*Capsicum annuum*) and two *Solanum habrochaites* (a tomato wild relative) inbred lines were used for infectivity tests. The pepper accessions had different alleles at the *pvr2* locus encoding eIF4E: Yolo Wonder was the susceptible reference carrying the *pvr2*⁺ allele, whereas Yolo Y, Florida VR2, HD285, PI322719, SC81, Maroc1, Serrano Vera Cruz, PI195301, and Chile de Arbol carried alleles *pvr2*¹ to *pvr2*⁹, respectively (7). These 10 alleles correspond to highly similar copies of an eIF4E which differ by a small number of amino acid substitutions (7, 12). The *S. habrochaites* accessions carried different alleles at the *pot-1* locus orthologous to the pepper *pvr2* locus: PI247087 carried the *pot-1* recessive resistance allele, whereas PI134417 was the susceptible reference (*pot-1*⁺) (13). Among all these resistance genes or alleles, only *pvr2*¹ and *pvr2*² are used extensively in breeding programs. They are present in 14% of 364 pepper cultivars registered in the European varietal catalogue between 1980 and 2010 (22% between 1990 and 2000) (A. Palloix, unpublished data).

Potato virus Y variants. Two sets of PVY variants were used: (i) viral populations derived from the two cDNA clones SON41p and LYE84 and from several of their VPg mutants (14, 15) and (ii) representative isolates collected from pepper crops corresponding to different haplotypes according to the VPg sequence. Four mutants of SON41p, named S101G, T115K, T115R, and D119N according to the position and nature of the amino acid substitution in the VPg, were obtained after experimental

	101	123
Alger1 (2007/Algeria/KF670573)	GEVRKKMVEDDEIGAQALSNNTR	
CAA14 (Tanzania/KF670570)	...M...K.G...ET...HA..N	
CAA141 (1999/Montfavet, France/KF670580)	S.....E.....Y..K	
CAA15 (origin unknown/KF670594)	S...Q...M.E..EK...GS..T	
CAA16 (Sicily, Italy/AJ507381)	S...R..I.....QR...DS..T	
EP03 (2003/Montfavet, France/HG973457)	S...R.....ET...NS..S	
GHB11 (2006/Ghar-el-Mehl, Tunisia/JF824723)	.Q..R..I.....QR...ES..S	
Hur1 (2004/Espelette, France/HG973455)	S...R...N.D.ET...GS..T	
Hur2 (2004/Espelette, France/HG973456)	SD.....EL...GS..T	
K4794 (1994/Kairouan, Tunisia/KF670576)	S...R.....ET...S..S	
LYE84 (1984/Canary islands, Spain/AJ439545)	S.....EM...HS..N	
Mart3 (2009/Martinique, France/KF670567)	S.....ET...NSH..S	
SON41p (1982/Montfavet, France/AJ439544)	S...R.....ET...DSH..S	
UTA9 (2006/Utique, Tunisia/JF824727)	S...R.....E.....HS..N	

FIG 2 Characteristics and VPg sequence of pepper PVY isolates used in the present study. The sequence alignment of the central part of the VPg (amino acid positions 101 to 123) is shown, with dots indicating the presence of the same amino acid as in the first sequence. Year of collection, place of collection, and accession number of the VPg-coding sequence are indicated, respectively, in parentheses.

evolution in HD285 carrying the *pvr2*³ resistance allele (14). A fifth mutant, S120C, was excluded because of its lack of stability and difficulty in obtaining a homogeneous inoculum. Each mutation was introduced into the SON41p clone by site-directed mutagenesis and shown to be sufficient for pathogenicity against *pvr2*³. Similarly, two VPg mutants of LYE84, named H119R and H119Y, were obtained after experimental evolution in PI247087 carrying the *pot-1* resistance allele, and each mutation was introduced into the LYE84 clone by site-directed mutagenesis (15; also the present study). Mutations H119R (15) and H119Y (this study) were shown to be sufficient for pathogenicity against *pot-1*.

The sequences of the VPg-coding regions of 57 PVY isolates collected from pepper crops were determined (references 12, 16, and 17 and the present study), and 12 haplotypes were observed based on the amino acid diversity in the region spanning positions 101 to 123, shown to be critical for pathogenicity toward eIF4E-mediated resistance (14, 16). A single isolate was chosen to represent each haplotype for infectivity tests (Fig. 2).

Analysis of the infectivity properties of PVY variants. Because direct bombardment of pepper or *S. habrochaites* plants with PVY cDNA was unsuccessful, we used *Nicotiana clevelandii* as a first host for cDNA bombardment. Then, the virus populations obtained from cDNA clones of SON41p, LYE84, and their six VPg mutants were inoculated mechanically onto plants representing 10 pepper and 2 *S. habrochaites* genotypes with different eIF4Es, as previously described (15). For SON41p and LYE84, inoculation of plants carrying recessive resistance genes or alleles was also performed after an additional passage of the virus population in plants of the susceptible pepper and *S. habrochaites* reference genotypes, respectively. The 12 representative PVY field isolates chosen as described above were inoculated mechanically onto the six pepper plants with genotypes featuring the *pvr2*¹, *pvr2*², *pvr2*³, *pvr2*⁵, or *pvr2*⁸ allele. The *pvr2*⁴ allele was not tested to avoid redundancy with *pvr2*³ (see the Results section), and the *pvr2*⁶, *pvr2*⁷, and *pvr2*⁹ alleles were not retained because plant accessions carrying these alleles were not (or rarely) infected by SON41p, LYE84, or their mutants (see the Results section). Symptoms were recorded from 2 to 5 weeks after inoculation, and PVY was detected by a double-antibody sandwich enzyme-linked immunosorbent assay (DAS-ELISA) and reverse transcription-PCR (RT-PCR) at 5 weeks after inoculation in apical leaves. At least two independent experiments, each comprising at least 20 plants per virus-plant genotype combination, were performed.

The nucleotide sequences of the VPg-coding regions of PVY populations that infected plants carrying resistance genes or of susceptible control plants were determined as described previously (12, 14) from a total of four (when available) infected plants per virus-plant genotype combination.

The H119Y mutation observed in the VPg-coding region of the PVY

TABLE 1 Nestedness and modularity of PVY-plant infectivity matrices

Parameter and algorithm	Value for the parameter in: ^a			
	PVY mutants		PVY isolates	
	Including susceptible plant genotypes	Excluding susceptible plant genotypes	Including susceptible plant genotypes	Excluding susceptible plant genotypes
Nestedness				
binmatnest2 ^b	0.80 (0.032* , 0.193)	0.71 (0.301, 0.541)	0.93 (0.021* , 0.106)	0.77 (0.340, 0.579)
NODF2 ^c	0.71 (0.011* , 0.172)	0.56 (0.231, 0.397)	0.85 (0.009** , 0.028*)	0.73 (0.128, 0.267)
WINE ^d	0.61 (0.011* , 0.117)	0.53 (0.059, 0.332)	0.64 (0.015* , 0.070)	0.47 (0.289, 0.400)
Modularity				
leading.eigenvector.community ^e	0.22 (0.371, 0.326)	0.25 (0.316, 0.292)	0.18 (0.374, 0.343)	0.19 (0.077, 0.255)
spinglass.community ^f	0.20 (NA, NA)	0.22 (NA, NA)	0.18 (NA, NA)	0.22 (NA, NA)
optimal.community ^g	0.23 (0.765, 0.516)	0.27 (0.433, 0.328)	0.18 (0.734, 0.468)	0.19 (0.107, 0.327)
edge.betweenness.community ^h	0.11 (0.527, 0.373)	0.25 (0.191, 0.178)	0	0
infomap.community ⁱ	0	0	0	0

^a Nestedness and modularity were estimated with different algorithms of the R software package, and estimation values are indicated separately for PVY VPg mutants or field isolates and including or excluding the *Capsicum annuum* and *Solanum habrochaites* susceptible reference genotype plants that were infected by all PVY variants (Fig. 1d and e). Values in parentheses are the frequencies of matrices simulated under the Bernoulli null model and the probabilistic degree null model, respectively, showing higher nestedness or modularity estimates than the experimental infectivity matrices, except when no module was detected (modularity indicated as 0). Totals of 10,000 (nestedness) or 1,000 (modularity) matrices were simulated independently under the two null models. Nestedness was significant at the 5% (*) and 1% (**) type I error threshold (in bold). NA, not available (the method cannot work with unconnected graphs, many of which were obtained in the matrices simulated under the null models).

^b R function according to Rodríguez-Gironés and Santamaría (19).

^c R function according to Almeida-Neto et al. (20).

^d R function according to Galeano et al. (21).

^e R function according to Newman (22).

^f R function according to Newman and Girvan (24), Reichardt and Bornholdt (25), and Traag and Bruggeman (26).

^g R function according to Brandes et al. (27).

^h R function according to Newman and Girvan (24).

ⁱ R function according to Rosvall and Bergstrom (28).

population infecting the PI247087 accession of *S. habrochaites* carrying the *pot-1* resistance gene after inoculation by LYE84 was introduced into the LYE84 cDNA clone by site-directed mutagenesis and homologous recombination in *Saccharomyces cerevisiae* as described by Ayme et al. (14).

Statistical analysis of the structure of virus-plant infectivity matrices. Three criteria were chosen to describe virus-plant infectivity matrices and to compare them to expectations of the GFG, MA, and modular models: (i) the total number of compatibility cases in the matrix, (ii) their nestedness, and (iii) their modularity. Methods to estimate nestedness and modularity are described in Weitz et al. (18). Nestedness varies usually from 0 (low nestedness) to 1 (high nestedness) and was estimated by three different algorithms (19–21) with the package bipartite of the R software program (<http://cran.r-project.org/>). Modularity reflects the concentration of compatibility cases within modules compared with random distribution regardless of modules (18, 22) and varies from –1 (antimodular matrix) to +1 (high modularity matrix). Values close to zero correspond to random partitions into modules of randomly distributed compatibility cases. Given the contrasts in statistical power to detect modules between methods (23), we used five different algorithms, implemented in the package igraph of the R software program to estimate modularity (22, 24–28) (Table 1). For statistical significance assessment, the nestedness and modularity of the plant-virus interaction matrices obtained experimentally (in brief experimental matrices) were compared to two different null models as described by Weitz et al. (18). In the first one (Bernoulli random null model), the same total number of compatibility cases as in the experimental matrices was randomly distributed in matrices containing the same number of rows and columns as the experimental matrices. In the second one (probabilistic degree null model), each plant virus combination in the matrix was assigned a probability of being a compatible interaction which was equal to the mean of the frequencies of compatibility cases in the same column and in the same row in the experimental matrix. One thousand (for modularity) or 10,000 (for nestedness)

simulations were performed for both null models. For all analyses, redundant or empty rows or columns (i.e., rows or columns sharing the same compatibility cases or containing no compatibility cases, respectively) were withdrawn.

RESULTS

Infectivity of PVY variants in *Capsicum annuum* and *Solanum habrochaites*. In a first set of experiments, plants of *C. annuum* and *S. habrochaites* representing genotypes with different alleles at the *pvr2* and *pot-1* locus, respectively, encoding highly similar eIF4E copies (7) were inoculated mechanically with virus populations produced from cDNA clones of isolates SON41p and LYE84 and of their VPg mutants (Fig. 1d). Mutants S101G, T115K, T115R, and D119N of SON41p had been selected by *C. annuum* accession HD285 plants carrying the resistance allele *pvr2*³, and mutants H119R and H119Y of LYE84 had been selected by *S. habrochaites* accession PI247087 plants carrying the resistance allele *pot-1*. Three categories of reactions were observed in plants at 5 weeks after inoculation. In 44% of plant-PVY combinations (42/96), 100% of plants were infected at the systemic level, and no additional mutation was observed in the VPg-coding region of the PVY populations. In 46% (44/96) of cases, no plant was infected at the systemic level. Finally, in 10% of cases (10/96), the infection frequency was below 100% (from 2.2 to 82.6%), and secondary nonsynonymous substitutions were always observed in the VPg-coding region of the PVY progeny (Fig. 1d). These secondary mutations were at codon positions 101, 105, 115, 119, 120, and 121 of the VPg, which were shown to determine pathogenicity toward the *pvr2* and/or *pot-1* gene (14–16). Concerning the mutations observed in the progeny of SON41p and LYE84 VPg mutants, the

responsibility of the identified secondary mutations in the VPg-coding region in determining infection was not formally established (this would have required introducing these mutations by site-directed mutagenesis into the cDNA clones of the PVY mutants). However, six of these PVY mutants carrying secondary mutations were randomly chosen for back-inoculation to the same plant genotype (Fig. 1d). For all of them, 100% (25 of 25) of plants were infected 15 days after inoculation, and no additional mutation was observed in the VPg-coding region of the viral progeny. This shows clearly that the infected plants of the latter category correspond to resistance breakdown (RB) events that occurred during the test and do not represent the initial infectivity properties of the PVY mutant. For this reason, plant-PVY combinations corresponding to this third category were considered incompatibility cases in analyses of the interaction patterns of infectivity matrices. Importantly, for all plant genotypes corresponding to this third category for the VPg mutants, no infection was observed after inoculation by the PVY populations derived from the initial cDNA clones (SON41p or LYE84), even after an additional passage in a pepper or *S. habrochaites* plant with the reference susceptibility genotype to produce the inocula, evidencing an evolutionary springboard effect conferred by the first acquired RB mutation (see below).

As a whole, plants with the reference susceptibility genotypes of *C. annuum* and *S. habrochaites* were 100% infected by all PVY variants. In contrast, none of the plants carrying *pvr2*⁶ or *pvr2*⁷ were infected. The *C. annuum* plants with genotype *pvr2*³ or *pvr2*⁴ showed the same behaviors toward all PVY variants. This is in accordance with the fact that they possess very similar eIF4E sequences, differing by a single amino acid substitution (7, 12), and suggests that they are redundant in terms of interaction specificity with PVY. In total, the PVY variants were able to infect plants belonging to 1 to 5 plant genotypes (3.25 on average) carrying resistance genes or alleles (i.e., excluding the reference susceptibility plant genotypes), of a total of 10, if we consider only cases where 100% of plants were infected.

In a second set of experiments, the six pepper plants with the *pvr2*⁺, *pvr2*¹, *pvr2*², *pvr2*³, *pvr2*⁵, or *pvr2*⁸ genotype were inoculated mechanically with 12 representative PVY field isolates corresponding to different haplotypes based on the amino acid diversity of the central part of the VPg, which determines pathogenicity toward recessive resistance genes in the *Solanaceae* (Fig. 1e). Results were quite similar to those obtained with SON41p, LYE84, and their VPg mutants. We observed the same three categories of reactions as previously for SON41p, LYE84, and their mutants. Again, the category where the infection frequency was below 100% and where secondary nonsynonymous substitutions were observed in the VPg-coding region of the PVY progeny corresponded to RB events that occurred during the test. Indeed, for eight randomly chosen PVY mutants carrying secondary mutations, 100% (25 of 25) of plants were infected 15 days after back-inoculation to the same plant genotype, and no additional mutation was observed in the VPg-coding region of the viral progeny (Fig. 1e). Compared to the previous experiment, a fourth category of reaction was observed in three PVY isolate-*pvr2* resistance allele combinations, with 100% infection and occurrence of amino acid substitutions in the VPg compared to the sequence of the virus from the inoculum or from susceptible reference plants. This category includes isolate CAA14 versus a *pvr2*⁸ plant and isolate CAA15 versus a *pvr2*¹ or *pvr2*⁵ plant (Fig. 1e). It is possible that

these isolates were only partly adapted to the resistance alleles, and their fitness was increased by the observed mutations. Alternatively, minor variants present in the PVY inoculum could have been selected during the experiment. All plants of the susceptible reference genotype were infected by all isolates. In contrast, none of the plants of the *pvr2*² genotype were infected. The isolates were able to infect plants belonging to 0 to 4 plant genotypes (1.58 on average) carrying *pvr2* resistance alleles (excluding the reference susceptibility plant genotype), of a total of 5, if we consider only cases where 100% plants were infected. This corresponds roughly to the same infectivity probability as with the PVY mutants, with a probability of 0.316 for PVY field isolates to infect plants carrying a *pvr2* resistance allele and of 0.325 for SON41p, LYE84, and their mutants.

Analysis of the interaction pattern between PVY variants and *Capsicum annuum* and *Solanum habrochaites*. The three proposed host-parasite interaction models (GFG, MA, and modular) are characterized by different frequencies of compatibility cases in infectivity matrices as well as different structures of these compatibility cases in terms of nestedness and modularity (Fig. 1a to c). The frequency of compatibility cases observed in our experimental matrices was much higher than that expected under the MA model ($P < 0.004$; Fisher's exact tests) but similar to that expected under the GFG model ($P > 0.34$; Fisher's exact tests). Results were similar for the matrices obtained with field isolates or VPg mutants of SON41p and LYE84 and keeping or excluding plants with susceptible *C. annuum* and *S. habrochaites* reference genotypes. Results were also highly consistent between the three nestedness estimation algorithms and between the five modularity estimation algorithms (Table 1). The experimental matrices obtained for the VPg mutants or the field isolates showed low modularity values (< 0.23) but high nestedness values (0.61 to 0.93) (Table 1; Fig. 1d and e). In addition, the experimental matrices were not more modular than matrices generated under the null models (at least 32.6% of the simulated matrices had higher modularity values than the experimental matrices). In contrast, the experimental matrices were significantly more nested than matrices generated under the Bernoulli null model (see Materials and Methods) (18) ($P = 0.009$ to 0.032, depending on the matrix and the algorithm). However, they were not, except in one case, significantly more nested than matrices generated under the probabilistic degree null model at the 5% error threshold. The rather marginal nestedness observed in the experimental matrices was also influenced by the presence of plants with the reference susceptibility genotypes, which were infected by all PVY variants, and neither nestedness nor modularity was significant if we considered only plant genotypes with resistance alleles.

DISCUSSION

The interaction patterns between PVY and pepper and *S. habrochaites* differ significantly from the matching allele or modular models. Interactions between plant and virus genotypes were proposed to correspond to the GFG or MA model on the basis of the structure of infectivity matrices and of the molecular mechanisms determining infectivity of the virus and resistance of the plant (4). However, plant-virus infectivity matrices have been only rarely determined and usually comprise only a small number of plant and/or virus genotypes, hampering any statistical analysis of their structure. Interaction between plants with genotypes harboring various alleles at eIF4E (or eIF4G)-encoding loci controlling sus-

ceptibility or recessive resistance and different groups of viruses were considered emblematic of the MA model (4). Indeed, in these systems, infection was shown to depend on a specific match and a direct physical interaction between the plant eIF4E (or eIF4G) and a virus pathogenicity factor, usually the VPg (7, 8). Mutations in the plant factor that abolish interaction with the virus VPg confer resistance to the plant, and mutations in the virus VPg that restore interaction with the mutated plant factor are responsible for infectivity of the virus in plants carrying resistance alleles. However, again, little data were available to support this model on the basis of the structure of the interaction matrix between plant and virus genotypes.

The infectivity matrices that we obtained with PVY clones and mutants or with field isolates and genotypes of *C. annuum* and *S. habrochaites* plants did not show any evidence of modularity, as would have been the case for the MA model or for a more relaxed modular model. This was mainly due to a high frequency of cross-infectivity, each PVY variant usually being able to infect plants representing several genotypes with different resistance alleles. However, even taking into account this high frequency of cross-infectivity, our experimental matrices were not more modular than matrices generated at random. The lack of modularity indicates that there is no tendency for PVY variants with similar VPgs to infect plants with similar eIF4Es (and vice versa). As a consequence, it is not possible to predict the infectivity properties of a given PVY isolate from those of its closest VPg sequence variants.

In contrast, significant nestedness was detected for some of our experimental matrices, which could be reminiscent of the GFG model of interaction. However, this effect was rather marginal, and the molecular mechanism of interaction between PVY and plants carrying recessive resistance alleles does not correspond to an elicitor-receptor interaction triggering specific plant defenses, as usually considered in the GFG model (3). It should be noted, however, that nested, but not modular, patterns of interaction were frequently detected in phage-bacteria interactions (29) and could be a rather general pattern of interaction.

The PVY-plant interaction considered here is consequently intermediate between the GFG and MA models, sharing the mechanistic bases of the MA model and the extensive cross-infectivity of the GFG model. One explanation could be that potyvirus VPgs possess intrinsically disordered domains, especially in the central part which corresponds to the pathogenicity determinant against recessive resistance genes (30–32), which can confer the ability to bind different ligands (33, 34) and/or to bind a large set of allelic forms of a given ligand like eIF4E. However, this structural flexibility has some limits, and, in contrast with the GFG model, we did not observe any PVY variant with universal infectivity (Fig. 1d and e).

In addition to this static view of the virus-plant interaction pattern at a given evolutionary time, it is also important to consider their genetic bases in a more dynamic view to unravel their causes and consequences. Remarkably, highly similar structural patterns of infectivity matrices were observed for SON41p, LYE84, and their mutants, on one hand (hence representing a very low virus genetic diversity), and for PVY isolates collected from pepper fields worldwide, on the other hand (hence, comprising a much larger genetic diversity). This suggests that the same genetic mechanisms could be involved in determining the observed interaction patterns.

Widespread cross-infectivity and evolutionary springboard effects of PVY mutations in solanaceous crops. The PVY VPg

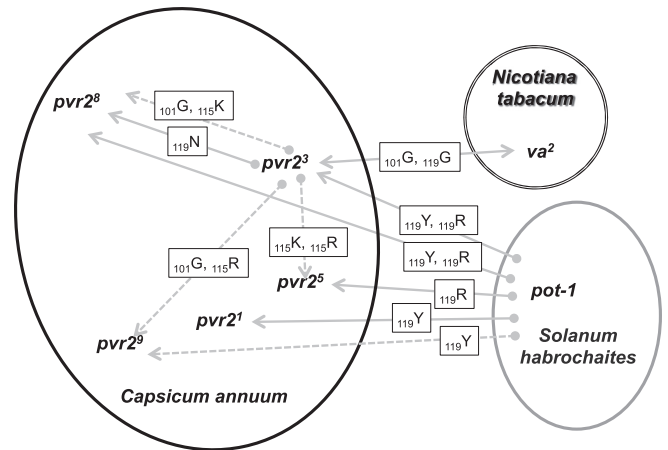


FIG 3 Cross-infectivity and springboard effects of PVY mutations involved in resistance breakdown (RB) in three solanaceous species. Arrows with solid lines correspond to cross-infectivity effects, and arrows with broken lines correspond to evolutionary springboard effects of RB mutations. Mutations in boxes correspond to amino acid substitutions in PVY VPg conferring RB. Arrows point toward the second resistance gene or allele for which cross-infectivity or springboard effects are observed after fixation of the mutation involved in the breakdown of a first resistance gene. The double-headed arrow indicates that the two considered resistance genes can select the mutation (symmetrical cross-infectivity).

mutants used in the present study were the results of experimental evolution of populations derived from the SON41p and LYE84 clones. Initially, SON41p was infectious only in pepper plants carrying *pvr2*¹ or *pvr2*² in addition to plants with the susceptibility alleles, and LYE84 was infectious only in plants with the susceptibility alleles. After a first set of inoculations, SON41p gained infectivity toward the *pvr2*³ resistance allele in pepper, and LYE84 gained infectivity toward the *pot-1* resistance allele in *S. habrochaites* (14, 15). These RBs were due to precise amino acid substitutions in the VPg (Fig. 1d). When the VPg mutants of SON41p and LYE84 were inoculated onto the set of plants carrying different eIF4E alleles, different kinds of pleiotropic effects were observed.

The first kind of pleiotropic effect can be named cross-infectivity by analogy to cross-resistance of microbes, insects, or weeds to different (bio)chemical compounds in a medical or agricultural context (35–39). It can be defined as the effect of a single mutational event which leads to the breakdown of at least two plant resistance genes or alleles, an initial one, which exerts selection pressure on the pathogen population leading to the fixation of an RB mutation, and a second one, which does not play any role in the fixation of the RB mutation. As best examples of cross-infectivity, the breakdown mutations selected by *pot-1* resistance in *S. habrochaites* resulted also in the breakdown of four distinct *pvr2* resistance alleles in pepper (Fig. 1d and 3). Similar cross-infectivity effects are also expected between tobacco (*Nicotiana tabacum*) and pepper resistance genes. Indeed, it was shown previously that the VPg of PVY was also the pathogenicity factor corresponding to the *va* gene in tobacco (40, 41). Sequence comparisons indicated that the S101G and D119G substitutions in the VPg of PVY SON41p allowed the breakdown of the *va*² resistance allele in tobacco. These two substitutions also allowed the breakdown of the *pvr2*³ allele (14, 42), displaying consequently a cross-infectivity effect between the *va*² and *pvr2*³ alleles in tobacco and pepper cultivars, respectively (Fig. 3). Obviously,

this definition is only meaningful if the two resistance genes considered have different specificities, i.e., different spectra of action toward the pathogen diversity. Since the *pvr2*³ and *pvr2*⁴ resistance alleles showed the same specificities of action toward the eight PVY clones and mutants tested (Fig. 1d), which is consistent with their sequence similarity (one amino acid difference only) (7), we would not define as cross-infectivity the effect of VPg mutations involved in the simultaneous breakdown of *pvr2*³ and *pvr2*⁴.

The second kind of pleiotropic effect, which we named the evolutionary springboard effect, occurs when a first plant resistance gene (or allele) leads to the fixation of a first RB mutational event in the virus population which further favors the breakdown of a second resistance gene (or allele) through an additional mutational event(s). In that case, the direct inoculation of the initial virus population (SON41p or LYE84) to plants carrying the second resistance gene did not lead to infection, even after a supplementary passage in susceptible reference plants before inoculation, evidencing the evolutionary springboard effect. As best examples of the springboard effect, mutations T115K and T115R that were selected by the *pvr2*³ resistance allele favored the breakdown of *pvr2*⁵ and *pvr2*⁸ and, respectively, of *pvr2*⁵ and *pvr2*⁹ (Fig. 1d and 3).

Cross-infectivity and springboard effects correspond to positive or synergistic pleiotropy effects, where a single mutation has two favorable effects for the pathogen, allowing infection of, or acquisition of, RB properties toward plant genotypes representing two different resistance genes or alleles. In contrast, the third case of pleiotropic effect identified in this study corresponds to antagonistic pleiotropy, where a mutation allows the breakdown of a first resistance gene and abolishes simultaneously the capacity of breakdown of a second one. Antagonistic pleiotropy was observed among PVY VPg mutations involved in the breakdown of alleles *pvr2*² and *pvr2*³ in pepper, such as mutations T115K, T115R, and D119N (Fig. 1d).

The ability of many field PVY isolates to infect pepper plants with different *pvr2* resistance alleles is likely the result of cross-infectivity effects of mutations. Only the *pvr2*¹ and *pvr2*² recessive resistance genes have been largely deployed worldwide. Whereas none of the isolates was able to infect *pvr2*² plants, six of them were breaking the *pvr2*¹ allele without the requirement of additional mutations in the VPg (Fig. 1e). Four of these isolates (Alger1, GHB11, CAA16, and CAA141) (15; also our unpublished data) were collected in plants homozygous for *pvr2*¹ (no data are available for the plant origin of the other two isolates). The selective cause of the *pvr2*¹-breaking capacity of these isolates was probably the *pvr2*¹ allele itself, and their capacity to infect plants having genotypes with other *pvr2* resistance alleles is the by-product of the fixation of the *pvr2*¹-breaking mutation. Supporting this assumption, the six isolates infecting pepper plants carrying the *pvr2*¹ genotype had a significantly higher capacity to infect pepper plants with additional genotypes than the six isolates that were not infecting the *pvr2*¹ pepper ($P = 0.005$; Fisher exact test). Unfortunately, it was impossible to reconstruct the mutational pathways leading to *pvr2*¹ breakdown for the former six isolates because of the large number of mutations at the amino acid positions critical for pathogenicity toward *pvr2* plants compared to isolates that did not break *pvr2*¹ (Fig. 2).

Such synergistic pleiotropic effects of infectivity mutations are rare in plant-pathogen interactions, and only a few cross-infectivity

effects have been described (11, 43–45). To our knowledge, no evolutionary springboard effect among RB mutations has been described so far. For example, in the most exhaustive study, only one of eight (12.5%) RB mutations in the VPg of RYMV conferred simultaneously the capacity to infect rice plants with the *rymv1*–2 and *rymv1*–3 resistance alleles, and 4 of 38 RYMV isolates (11%) were infectious in both kinds of rice genotypes (11), showing the rarity of cross-infectivity in this system. However, such effects could have been underestimated because of the small size of the plant-pathogen interaction matrices usually analyzed. In comparison, in our system, we observed seven occurrences of cross-infectivity effects and seven of evolutionary springboard effects (Fig. 3), which represents 17.5% for each if we include the *pvr2*⁶ and *pvr2*⁷ alleles (7 of 40 combinations between VPg mutations and *pvr2* alleles that could reveal pleiotropic effects).

Consequences on resistance management strategies. Evaluating whether mutations involved in the breakdown of different plant resistance genes or alleles are independent or not is crucial since it determines the risk of emergence of multivirulent pathogens (i.e., pathogens breaking down simultaneously the resistance controlled by several genes or alleles) and the sustainability of disease control strategies based on genetic resistance (46, 47). In this respect, the evolutionary pathways leading to multivirulence and the different cases of pleiotropic effects of RB mutations (cross-infectivity, evolutionary springboards, and antagonistic pleiotropy) determine the probability of emergence of RB populations (47, 48).

Cross-infectivity and springboard effects are likely to decrease the efficiency of resistance management strategies such as varietal rotations or mixtures. The fact that these effects occur also between different plant species and even genera like *Nicotiana*, *Solanum*, and *Capsicum* (Fig. 3) indicates that the different crop species in the agricultural landscape should be considered simultaneously in this regard. Wolfe (49) reviewed four mechanisms by which growing mixtures of plant cultivars carrying different resistance genes or alleles in the same fields increased resistance durability: (i) the decrease of host density for the pathogen, compared to situations with 100% susceptible plants (or plants in which resistance is broken down), (ii) the barrier effect reducing transmission efficiency due to nonhosts, (iii) the counterselection of RB mutations through the fitness costs of these mutations in hosts lacking the corresponding resistance, and (iv) the decrease of selection pressure for RB variants compared to situations with 100% of plants carrying the resistance gene. The same four mechanisms are also in play during rotation strategies if we take into account several consecutive cropping seasons. Cross-infectivity and springboard effects will suppress or decrease the action of these four mechanisms and are therefore expected to reduce drastically the efficiency of the mixture and rotation strategies. Indeed, a pathogen isolate carrying cross-infectivity mutations (or showing evolutionary springboard effects) will be able to infect (or to evolve RB capacity toward) a larger panel of cultivars in the mixture, hence increasing its host density (mechanism i) and reducing the barrier effects (mechanism ii). Also, several cultivars in the mixture will contribute to select and maintain the same RB mutations in the pathogen population, in the case of both cross-infectivity and evolutionary springboard effects, which will reduce the effects of counterselection (mechanism iii) and of decreased selection pressure (mechanism iv).

ACKNOWLEDGMENTS

We thank Joël Chadœuf (INRA PACA) for helpful discussions about estimations of nestedness and modularity and Josselin Montarry (INRA Rennes) for improving the manuscript.

This work was supported by the SYSTERRA program of the Agence Nationale de la Recherche, a French-Tunisian PHC Utique bilateral project (10G0905), and a project from the Maladies Infectieuses Emergentes interdisciplinary program of the Centre National de la Recherche Scientifique.

REFERENCES

- Luijckx P, Fienberg H, Duneau D, Ebert D. 2013. A matching-allele model explains host resistance to parasites. *Curr. Biol.* 23:1085–1088. <http://dx.doi.org/10.1016/j.cub.2013.04.064>.
- Gandon S, Capowiez Y, Dubois Y, Michalakakis Y, Olivieri I. 1996. Local adaptation and gene-for-gene coevolution in a metapopulation model. *Proc. Biol. Sci.* 263:1003–1009. <http://dx.doi.org/10.1098/rspb.1996.0148>.
- Dybdahl MF, Storfer A. 2003. Parasite local adaptation: Red Queen versus Suicide King. *Trends Ecol. Evol.* 18:523–530. [http://dx.doi.org/10.1016/S0169-5347\(03\)00223-4](http://dx.doi.org/10.1016/S0169-5347(03)00223-4).
- Sacristán S, García-Arenal F. 2008. The evolution of virulence and pathogenicity in plant pathogen populations. *Mol. Plant Pathol.* 9:369–384. <http://dx.doi.org/10.1111/j.1364-3703.2007.00460.x>.
- Agrawal A, Lively CM. 2002. Infection genetics: gene-for-gene versus matching-alleles models and all points in between. *Evol. Ecol. Res.* 4:79–90.
- Fraile A, Pagan I, German A, Saez E, García-Arenal F. 2011. Rapid genetic diversification and high fitness penalties associated with pathogenicity evolution in a plant virus. *Mol. Biol. Evol.* 28:1425–1437. <http://dx.doi.org/10.1093/molbev/msq327>.
- Charron C, Nicolai M, Gallois JL, Robaglia C, Moury B, Palloix A, Caranta C. 2008. Natural variation and functional analyses provide evidence for co-evolution between plant eIF4E and potyviral VPg. *Plant J.* 54:56–68. <http://dx.doi.org/10.1111/j.1365-313X.2008.03407.x>.
- Hébrard E, Poulicard N, Gérard C, Traore O, Wu HC, Albar L, Fargette D, Bessin Y, Vignols F. 2010. Direct interaction between the *Rice yellow mottle virus* (RYMV) VPg and the central domain of the rice eIF(iso)4G1 factor correlates with rice susceptibility and RYMV virulence. *Mol. Plant Microbe Interact.* 23:1506–1513. <http://dx.doi.org/10.1094/MPMI-03-10-0073>.
- Poulicard N, Pinel-Galzi A, Traoré O, Vignols F, Ghesquière A, Konate G, Hébrard E, Fargette D. 2012. Historical contingencies modulate the adaptability of *Rice yellow mottle virus*. *PLoS Pathog.* 8:e1002482. <http://dx.doi.org/10.1371/journal.ppat.1002482>.
- Pinel-Galzi A, Rakotomalala M, Sangu E, Sorho F, Kanyeka Z, Traoré O, Sérémié D, Poulicard N, Rabenantoandro Y, Séré Y, Konaté G, Ghesquière A, Hébrard E, Fargette D. 2007. Theme and variations in the evolutionary pathways to virulence of an RNA plant virus species. *PLoS Pathog.* 3:e180. <http://dx.doi.org/10.1371/journal.ppat.0030180>.
- Traoré O, Pinel-Galzi A, Issaka S, Poulicard N, Aribi J, Ake S, Ghesquière A, Séré Y, Konate G, Hébrard E, Fargette D. 2010. The adaptation of *Rice yellow mottle virus* to the eIF(iso)4G-mediated rice resistance. *Virology* 408:103–108. <http://dx.doi.org/10.1016/j.virol.2010.09.007>.
- Moury B, Charron C, Janzac B, Simon V, Gallois J-L, Palloix A, Caranta C. 3 December 2013. Evolution of plant eukaryotic initiation factor 4E (eIF4E) and potyvirus genome-linked viral protein (VPg): a game of mirrors impacting resistance spectrum and durability. *Infect. Genet. Evol.* <http://dx.doi.org/10.1016/j.meegid.2013.11.024>.
- Ruffel S, Gallois JL, Lesage ML, Caranta C. 2005. The recessive potyvirus resistance gene *pot-1* is the tomato orthologue of the pepper *pvr2*-eIF4E gene. *Mol. Genet. Genomics* 274:346–353. <http://dx.doi.org/10.1007/s00438-005-0003-x>.
- Ayme V, Souche S, Caranta C, Jacquemond M, Chadœuf J, Palloix A, Moury B. 2006. Different mutations in the genome-linked protein VPg of *Potato virus Y* confer virulence on the *pvr2*³ resistance in pepper. *Mol. Plant Microbe Interact.* 19:557–563. <http://dx.doi.org/10.1094/MPMI-19-0557>.
- Moury B, Morel C, Johansen E, Guilbaud L, Souche S, Ayme V, Caranta C, Palloix A, Jacquemond M. 2004. Mutations in *Potato virus Y* genome-linked protein determine virulence toward recessive resistances in *Capsicum annuum* and *Lycopersicon hirsutum*. *Mol. Plant Microbe Interact.* 17:322–329. <http://dx.doi.org/10.1094/MPMI.2004.17.3.322>.
- Ayme V, Petit-Pierre J, Souche S, Palloix A, Moury B. 2007. Molecular dissection of the *Potato virus Y* VPg virulence factor reveals complex adaptations to the *pvr2* resistance allelic series in pepper. *J. Gen. Virol.* 88:1594–1601. <http://dx.doi.org/10.1099/vir.0.82702-0>.
- Ben Khalifa M, Simon V, Fakhfakh H, Moury B. 2012. Tunisian *Potato virus Y* isolates with unnecessary pathogenicity towards pepper: support for the matching allele model in eIF4E resistance-potyvirus interactions. *Plant Pathol.* 61:441–447. <http://dx.doi.org/10.1111/j.1365-3059.2011.02540.x>.
- Weitz JS, Poisot T, Meyer JR, Flores CO, Valverde S, Sullivan MB, Hochberg ME. 2013. Phage-bacteria infection networks. *Trends Microbiol.* 21:82–91. <http://dx.doi.org/10.1016/j.tim.2012.11.003>.
- Rodríguez-Gironés MA, Santamaría L. 2006. A new algorithm to calculate the nestedness temperature of presence-absence matrices. *J. Biogeogr.* 33:924–935. <http://dx.doi.org/10.1111/j.1365-2699.2006.01444.x>.
- Almeida-Neto M, Guimaraes P, Guimaraes PR, Loyola RD, Ulrich W. 2008. A consistent metric for nestedness analysis in ecological systems: reconciling concept and measurement. *Oikos* 117:1227–1239. <http://dx.doi.org/10.1111/j.0030-1299.2008.16644.x>.
- Galeano J, Pastor JM, Iriando JM. 2008. Weighted-interaction nestedness estimator (WINE): a new estimator to calculate over frequency matrices. *Environ. Model. Softw.* 24:1342–1346. <http://dx.doi.org/10.1016/j.envsoft.2009.05.014>.
- Newman ME. 2006. Modularity and community structure in networks. *Proc. Natl. Acad. Sci. U. S. A.* 103:8577–8582. <http://dx.doi.org/10.1073/pnas.0601602103>.
- Aldecoa R, Marín I. 2013. Exploring the limits of community detection strategies in complex networks. *Sci. Rep.* 3:2216. <http://dx.doi.org/10.1038/srep02216>.
- Newman ME, Girvan M. 2004. Finding and evaluating community structure in networks. *Phys. Rev. E Stat. Nonlin. Soft Matter Phys.* 69:026113. <http://dx.doi.org/10.1103/PhysRevE.69.026113>.
- Reichardt J, Bornholdt S. 2006. Statistical mechanics of community detection. *Phys. Rev. E Stat. Nonlin. Soft Matter Phys.* 74:016110. <http://dx.doi.org/10.1103/PhysRevE.74.016110>.
- Traag VA, Bruggeman J. 2009. Community detection in networks with positive and negative links. *Phys. Rev. E Stat. Nonlin. Soft Matter Phys.* 80:036115. <http://dx.doi.org/10.1103/PhysRevE.80.036115>.
- Brandes U, Delling D, Gaertler M, Gorke R, Hoefer M, Nikoloski Z, Wagner D. 2008. On modularity clustering. *IEEE Trans. Knowl. Data Eng.* 20:172–188. <http://dx.doi.org/10.1109/TKDE.2007.190689>.
- Rosvall M, Bergstrom CT. 2008. Maps of information flow reveal community structure in complex networks. *Proc. Natl. Acad. Sci. U. S. A.* 105:1118–1123. <http://dx.doi.org/10.1073/pnas.0706851105>.
- Flores CO, Meyer JR, Valverde S, Farr L, Weitz JS. 2011. Statistical structure of host-phage interactions. *Proc. Natl. Acad. Sci. U. S. A.* 108:E288–E297. <http://dx.doi.org/10.1073/pnas.1101595108>.
- Grzela R, Szolajska E, Ebel C, Madern D, Favier A, Wojtal I, Zagorski W, Chroboczek J. 2008. Virulence factor of *Potato virus Y* genome-attached terminal protein VPg is a highly disordered protein. *J. Biol. Chem.* 283:213–221. <http://dx.doi.org/10.1074/jbc.M705666200>.
- Hébrard E, Bessin Y, Michon T, Longhi S, Uversky VN, Delalande F, Van Dorsselaer A, Romero R, Walter J, Declerk N, Fargette D. 2009. Intrinsic disorder in viral proteins genome-linked: experimental and predictive analyses. *Virology* J. 6:23. <http://dx.doi.org/10.1186/1743-422X-6-23>.
- Rantalainen KI, Uversky VN, Permi P, Kalkkinen N, Dunker AK, Makinen K. 2008. Potato virus A genome-linked protein VPg is an intrinsically disordered molten globule-like protein with a hydrophobic core. *Virology* 377:280–288. <http://dx.doi.org/10.1016/j.virol.2008.04.025>.
- Elena SF, Rodrigo G. 2012. Towards an integrated molecular model of plant-virus interactions. *Curr. Opin. Virol.* 2:719–724. <http://dx.doi.org/10.1016/j.coviro.2012.09.004>.
- Jiang J, Laliberté J-F. 2011. The genome-linked protein VPg of plant viruses—a protein with many partners. *Curr. Opin. Virol.* 1:347–354. <http://dx.doi.org/10.1016/j.coviro.2011.09.010>.
- George AM. 1996. Multidrug resistance in enteric and other Gram-negative bacteria. *FEMS Microbiol. Lett.* 139:1–10. <http://dx.doi.org/10.1111/j.1574-6968.1996.tb08172.x>.
- Han HP, Yu Q, Purba E, Li M, Walsh M, Friesen S, Powles SB. 2012. A novel amino acid substitution Ala-122-Tyr in ALS confers high-level and broad resistance across ALS-inhibiting herbicides. *Pest Manag. Sci.* 68:1164–1170. <http://dx.doi.org/10.1002/ps.3278>.
- Mainardi JL, Villet R, Bugg TD, Mayer C, Arthur M. 2008. Evolution of peptidoglycan biosynthesis under the selective pressure of antibiotics in

- Gram-positive bacteria. *FEMS Microbiol. Rev.* 32:386–408. <http://dx.doi.org/10.1111/j.1574-6976.2007.00097.x>.
38. Race E. 2001. Cross-resistance within the protease inhibitor class. *Antivir. Ther.* 6(Suppl 2):29–36.
 39. Tabashnik BE, Unnithan GC, Masson L, Crowder DW, Li X, Carriere Y. 2009. Asymmetrical cross-resistance between *Bacillus thuringiensis* toxins Cry1Ac and Cry2Ab in pink bollworm. *Proc. Natl. Acad. Sci. U. S. A.* 106:11889–11894. <http://dx.doi.org/10.1073/pnas.0901351106>.
 40. Masuta C, Nishimura M, Morishita H, Hataya T. 1999. A single amino acid change in viral genome-associated protein of *Potato virus Y* correlates with resistance breaking in “virgin A mutant” tobacco. *Phytopathology* 89:118–123. <http://dx.doi.org/10.1094/PHYTO.1999.89.2.118>.
 41. Lacroix C, Glais L, Verrier JL, Jacquot E. 2011. Effect of passage of a *Potato virus Y* isolate on a line of tobacco containing the recessive resistance gene *va*² on the development of isolates capable of overcoming alleles 0 and 2. *Eur. J. Plant Pathol.* 130:259–269. <http://dx.doi.org/10.1007/s10658-011-9751-0>.
 42. Montarry J, Doumayrou J, Simon V, Moury B. 2011. Genetic background matters: a plant-virus gene-for-gene interaction is strongly influenced by genetic contexts. *Mol. Plant Pathol.* 12:911–920. <http://dx.doi.org/10.1111/j.1364-3703.2011.00724.x>.
 43. Abdul-Razzak A, Guiraud T, Peypelut M, Walter J, Houvenaghel MC, Candresse T, Le Gall O, German-Retana S. 2009. Involvement of the cylindrical inclusion (CI) protein in the overcoming of an eIF4E-mediated resistance against Lettuce mosaic potyvirus. *Mol. Plant Pathol.* 10:109–113. <http://dx.doi.org/10.1111/j.1364-3703.2008.00513.x>.
 44. Houterman PM, Cornelissen BJ, Rep M. 2008. Suppression of plant resistance gene-based immunity by a fungal effector. *PLoS Pathog.* 4:e1000061. <http://dx.doi.org/10.1371/journal.ppat.1000061>.
 45. Parlange F, Daverdin G, Fudal I, Kuhn ML, Balesdent MH, Blaise F, Grezes-Beset B, Rouxel T. 2009. *Leptosphaeria maculans* avirulence gene *AvrLm4-7* confers a dual recognition specificity by the *Rlm4* and *Rlm7* resistance genes of oilseed rape and circumvents *Rlm4*-mediated recognition through a single amino acid change. *Mol. Microbiol.* 71:851–863. <http://dx.doi.org/10.1111/j.1365-2958.2008.06547.x>.
 46. Mundt CC. 1990. Probability of mutation to multiple virulence and durability of resistance gene pyramids. *Phytopathology* 80:221–223. <http://dx.doi.org/10.1094/Phyto-80-221>.
 47. Fabre F, Bruchou C, Palloix A, Moury B. 2009. Key determinants of resistance durability to plant viruses: Insights from a model linking within- and between-host dynamics. *Virus Res.* 141:140–149. <http://dx.doi.org/10.1016/j.virusres.2008.11.021>.
 48. Fabre F, Montarry J, Coville J, Senoussi R, Simon V, Moury B. 2012. Modelling the evolutionary dynamics of viruses within their hosts: a case study using high-throughput sequencing. *PLoS Pathog.* 8:e1002654. <http://dx.doi.org/10.1371/journal.ppat.1002654>.
 49. Wolfe MS. 1985. The current status and prospects of multiline cultivars and variety mixtures for disease resistance. *Annu. Rev. Phytopathol.* 23: 251–273. <http://dx.doi.org/10.1146/annurev.py.23.090185.001343>.